Quantum Information Review
An International Journal

http://dx.doi.org/10.12785/qir/010202

Geometric phase as entanglement probe in a pumped three-level atom placed near a dielectric

M. S. Ateto[1,2,*]

[1] Mathematics Department, Faculty of Science at Qena, South Valley University, 83523 Qena, Egypt
[2] Mathematics Department, Faculty of Science, Gazan University, Gazan, Kingdom of Saudi Arabia

Received: 10 Feb. 2013, Revised: 15 Jun. 2013, Accepted: 18 Jun. 2013
Published online: 1 Jul. 2013

Abstract: We introduce new features of the connection between entanglement induced by interaction and geometric phase acquired by a composite quantum system. Geometric phase, that reflects Bell angle between input and output photons in atom-cavity interaction, for a bipartite system under the inuence of a dielectric of Lorentzian permittivity, is examined. We show that, with adjustment of Bell angle, typical features of atom-cavity entanglement can be obtained by considering a three- level appropriately positioned with respect to macroscopic bodies. We find that, due to the strong non-Markovian memory effects, phase Rabi oscillations, a principal signature of strong symmetrically or antisymmetrically photons evolution, are stimulated with atom farther from a medium with low oscillation frequency. On death of Rabi oscillations, which means symmetric entangled photons, a strong long-time-scale atom-cavity entanglement can be produced, specially, below the band gap region where the radiative decay dominates. This feature conicts the case of pure vacuum where atom-cavity entanglement decays exponentially. The feature that, our system is acting as a beam splitter (BS), is also, in detail, discussed. The results are of strong applications in construction of the universal quantum logic gates.

Keywords: Geometric phase, Entanglement, Three-level atom, Bell angle, Vacuum field, dielectric media, spontaneous decay rate, lineshift.

1 Introduction

It has long been realized that the decay rate of an excited atom is not an immutable property, but that it can be modified by the cavity mode structure [1,2]. Generally called the Purcell effect[1], the phenomenon is qualitatively explained by the fact that the local environment modies the strength and distribution of the vacuum electromagnetic modes with which the atom can interact, resulting indirectly in the alteration of atomic spontaneous emission properties. The possibility to control atomic spontaneous emission was shown theoretically for various cavity structures [3,4,5,6,7], optical fibers [8], photonic crystals [9], semiconductor quantum dots [10]. From statistical mechanics it is clear that dissipation is unavoidably connected with the appearance of a random force which gives rise to an additional noise source of the electromagnetic field. Hence, any quantum theory that is based on the assumption of a real permittivity can only be valid for narrow-bandwidth fields far from medium resonances where absorption can safely be disregarded. In experiments, however, using optical instruments (dielectrics-matters), such as beam splitters or cavities, requires careful examination with regard to their action on the light under study. Thus, depending on the specic configuration of inhomogeneities, the atomic spontaneous decay rate may both increase or decrease compared with that of the same atom placed in free space according to the modications in the photonic density of states due to the presence of dielectric-bodies[3]. This is the result of non-Markovian memory effects arising from the frequency variation of the photonic density of states near the dielectric [4,6]. In this letter we have two essentials aims: first, we wish to shed light on the relationship between geometric phase and entanglement in term of such a modified distribution of the vacuum electromagnetic modes. Second, answer the important question: can the unusual vacuum help on the generation of entanglement between the system parts for sufficiently long time. Generation of entanglement [11] in quantum systems has been a subject of intense theoretical and

* Corresponding author e-mail: mohammed.ateto@gmail.com; mohamed.ali11@sci.svu.edu.eg

experimental study motivated by both the fundamental issue and potential applications in quantum-information processing tasks [12]. In order to implement those tasks, one hopes that entanglement needed to be maintained for sufficiently long time to fulfill the design. Usually attempts are made to minimize the environmental effects [13,14,15,16,17]. Quite counterintuitively, in certain situations one can take advantage of the spontaneous emission for entanglement generation [18]. Moreover, entanglement is connected to the geometric phase (GP), acquired by cyclic or non-cyclic adiabatic evolutions. It found that, because of entanglement, the geometric phase is very different from that of the non-entangled case [19].
In the last ten years, a major thrust of many proposals have been devoted for the exploration of the connection between GPs and entanglement [19,20,21,22,23,24,25,26,27], due to its strong applications in the quantum information processing and quantum computation [28], specially in the construction of the universal quantum logic gates [29]. It was the first time to introduce the concept of GP by Pancharatnam [30] in his study of interference of light in distinct states of polarization. Its quantal counterpart was discovered by Berry [31], who proved the existence of GP in cyclic adiabatic evolutions. This was generalized to the case of nonadiabatic [32] and noncyclic [33] evolutions. Since the GP for a pure state is a nonintegrable quantity and depends only on the geometry of the path traced in the projective Hilbert space, it acts as a memory of a quantum system. Geometric phase [34] is one of the few approaches by which one may realize fault tolerant [28] quantum computation in addition to the fact that it is resilient to decoherence [35].

However, bipartite system is of great importance in quantum computation, such as the transfer of quantum information, the construction of entanglement as well as the realizations of logic operations. GPs have been studied for entangled bipartite systems. These include qubits precessing in magnetic fields [23] and general evolution[25] both without interaction (fixed entanglement) and various specic Hamiltonians for bipartite systems with interactions (changing entanglement) [36,37]. It has been shown [23,25] in bipartite systems that even if there are no interactions during the evolution, fixed entanglement affects the geometric phase. These facts together give rise to a question about the way by which entanglement can affect the GP and its motion in bipartite systems under the inuence of neighboring dielectrics. Many authors [23,24,25] have focus on the entanglement dependence of the geometric phase for subsystem and the coupling effect on the geometric phase for subsystem under adiabatic evolution. In Ref.[38], the authors proposed an efficient scheme for implementation of two-qubit nonconventional geometric quantum gates, based on a dissipative large-detuning interaction of two three-level atoms with a cavity mode is initially in the vacuum state. To the best of our knowledge, the treatment of such problem within the framework of exact quantum electrodynamics (QED) in dispersing and absorbing media, has so far never been considered in references. A much richer range of phenomena is to be expected when allowing for the presence of dispersing and absorbing media, where a complex interplay of the electric properties of the atom and the bodies influences the functional dependence of the atom-eld interaction. Our approach, which has the advantage of being simple and applicable to different congurations of three-level systems, renders general expressions for the three-atom wave vector, as shown in Secs. II-IV. A denition to both Berry phase and entanglement measure we are going to use is given in Secs. V and VI, respectively. In Sec. VII, applications to the general results are examined for an atom placed in free space as well as in front of a dielectric half-space including our numerical calculation and discussion are also reported. A summary and conclusions are given in Sec. VIII.

2 General Formalism

For an atom at a given position $\mathbf{r}_A$ that interacts with the electromagnetic eld in the presence of a dispersing and absorbing dielectric medium, in the electric dipole approximation, the overall system can be described by the multi-polar coupling Hamiltonian[3,39],

$$\hat{H} = \int d^3\mathbf{r} \int_0^\infty d\omega\, \hbar\omega\, \hat{\mathbf{f}}^\dagger(\mathbf{r},\omega)\cdot\hat{\mathbf{f}}(\mathbf{r},\omega)$$

$$+\sum_k \hbar\omega_k \hat{S}_{Akk} - \hat{\mathbf{d}}_A\cdot\hat{\mathbf{E}}(\mathbf{r}_A) \qquad (1)$$

Here, the bosonic fields $\hat{\mathbf{f}}(\mathbf{r},\omega)$ and $\hat{\mathbf{f}}^\dagger(\mathbf{r},\omega)$ are canonically conjugate variables of the system which consists of the electromagnetic field and body (including the dissipative system responsible for absorption) and satisfy the well-known commutation relations

$$\left[\hat{\mathbf{f}}_m(\mathbf{r},\omega),\hat{\mathbf{f}}_n^\dagger(\mathbf{r}',\omega')\right] = \delta_{mn}\delta(\omega-\omega')\delta(\mathbf{r}-\mathbf{r}') \qquad (2)$$

$$\left[\hat{\mathbf{f}}_m(\mathbf{r},\omega),\hat{\mathbf{f}}_n(\mathbf{r}',\omega')\right] = \left[\hat{\mathbf{f}}_m^\dagger(\mathbf{r},\omega),\hat{\mathbf{f}}_n^\dagger(\mathbf{r}',\omega')\right] = 0. \qquad (3)$$

where, the $\hat{S}_{Akk'} \equiv |k\rangle_{AA}\langle k'|$ are the atomic flip operators for the atom with $|k\rangle_A$ being the energy eigenstate of the atom, and $\hat{\mathbf{d}}_A = \sum_{k,k'}\hat{\mathbf{d}}_{Akk'}\hat{S}_{Akk'}$ is the electric dipole-moment operator of the atom ($\hat{\mathbf{d}}_{Akk'} =_A \langle k|\hat{\mathbf{d}}_A|k'\rangle_A$).
Further, the operator of the medium-assisted electric field operator $\hat{\mathbf{E}}(\mathbf{r})$ in terms of the variables $\hat{\mathbf{f}}(\mathbf{r},\omega)$ and $\hat{\mathbf{f}}^\dagger(\mathbf{r},\omega)$ as follows:

$$\hat{\mathbf{E}}(\mathbf{r}) = \int_0^\infty d\omega\, \hat{\mathbf{E}}(\mathbf{r},\omega) + \text{h.c.}, \qquad (4)$$

$$\hat{\mathbf{E}}(\mathbf{r},\omega) = i\sqrt{\tfrac{\hbar}{\varepsilon_0\pi}}\,\tfrac{\omega^2}{c^2}\int d^3\mathbf{r}'\sqrt{\varepsilon_I(\mathbf{r}',\omega)}\;\boldsymbol{G}(\mathbf{r},\mathbf{r}',\omega)\;.\;\hat{\mathbf{f}}(\mathbf{r}',\omega) \tag{5}$$

where $\boldsymbol{G}(\mathbf{r},\mathbf{r}',\omega)$ is the classical Green tensor satisfying the equation

$$\left[\frac{\omega^2}{c^2}\varepsilon(\mathbf{r},\omega) - \nabla\times\nabla\times\right]\boldsymbol{G}(\mathbf{r},\mathbf{r}',\omega) = -\delta(\mathbf{r}-\mathbf{r}') \tag{6}$$

and satisgfies the boundary condition at infinity, i. e.,

$$\boldsymbol{G}(\mathbf{r},\mathbf{r}',\omega)\to 0 \;\text{ if }\; |\,\mathbf{r}-\mathbf{r}'\,|\to\infty. \tag{7}$$

with spatially varying complex permittivity $\varepsilon(\mathbf{r},\omega) = \mathrm{Re}\varepsilon(\mathbf{r},\omega) + \mathrm{iIm}\varepsilon(\mathbf{r},\omega)$ by which the dielectric body is expressed.

3 Dynamic of A Pumped Three-Level Λ-Type Atom

Consider a Λ-type three-level atom located at a distance z_A from a surface of one-dimensional infinitely long single-wall dielectric layer. We assume that the atomic transition $|2\rangle\to|3\rangle$ is strongly coupled to the eld modes via the dipole $\hat{\mathbf{d}}_{23}$. Moreover, an external (classical) pump eld, with initial phase ϕ_L , frequency ω_L and intensity described by the Rabi frequency Ω_L , is applied to the atomic transition $|1\rangle\to|2\rangle$. The study of the influence of external fields is key issue because using driving elds one can reach high level of control of the systems state. The one-dimensional version of the Hamiltonian (1) in the rotating-wave approximation reads

$$\hat{H} = \int dz\int_0^\infty d\omega\;\hbar\omega\;\hat{f}^\dagger(r,\omega)\;\hat{f}(r,\omega) + \hbar\omega_0\hat{S}_{22}$$

$$-\left[d_{23}\hat{S}_{23}\hat{E}^{(+)}(z_A) + \mathrm{H.c.}\right] - \frac{\hbar\Omega_L}{2}\left[\hat{S}_{21}\,e^{-i(\vartheta_L+\omega_L t)} + \mathrm{H.c.}\right] \tag{8}$$

4 Equation of Motion

For the atom at time $t=0$ is prepared in a superposition of its two classically pumped levels $|1\rangle\to|2\rangle$,

$$|\,\psi(0)\rangle = C_1(0)\,|\,1\rangle + C_2(0)\,|\,2\rangle \tag{9}$$

where the rest of the system, that consists of the electromagnetic field and the medium, is in vacuum, $\rangle\,|\,\{0\}\rangle$, the state vector of the overall system at later time $t\geq 0$ can be expanded as

$$|\,\psi(t)\rangle = C_1(t)\,|\,1\rangle\,|\,\{0\}\rangle + C_2(t)\,e^{-i\omega_0 t}\,|\,2\rangle\,|\,\{0\}\rangle$$

$$+\int dz\int_0^\infty d\omega\,C_3(z,\omega,t)\,e^{-i\omega t}\,|\,3\rangle\;\hat{f}^\dagger(z,\omega)\,|\,\{0\}\rangle \tag{10}$$

where we assumed that the frequencies of the atomic transitions $|2\rangle\to|1\rangle$ and $|2\rangle\to|3\rangle$ are the same; $\omega_{21} = \omega_{23} = \omega_0$ and $\hat{f}^\dagger(z,\omega)\;|\;\{0\}\rangle$ represents the single-quantum excited state of the combined field-medium system. It is not difficult to prove that the Schrödinger equation for $|\psi(t)\rangle$ leads to the following system of (integro-)differential equations for the probability amplitudes $C_1(t), C_2(t)$ and $C_3(z,\omega,t)$ as

$$\dot{C}_1(t) = i\frac{\Omega_L}{2}e^{i\vartheta_L}\;e^{i\Delta_L t}C_2(t) \tag{11}$$

$$\dot{C}_2(t) = i\tfrac{\Omega_L}{2}e^{-i\vartheta_L}\;e^{-i\Delta_p t}C_1(t) - \tfrac{d_{23}}{\sqrt{\hbar\varepsilon_0\pi}}\int dz\int_0^\infty d\omega\,\tfrac{\omega^2}{c^2}\sqrt{\mathrm{Im}\varepsilon(z,\omega)}$$

$$\boldsymbol{G}(z_A,z,\omega)\;C_3(z,\omega,t)\;e^{-i(\omega-\omega_0)t} \tag{12}$$

$$\dot{C}_3(z,\omega,t) = \frac{d_{32}}{\sqrt{\hbar\varepsilon_0\pi}}\,\frac{\omega^2}{c^2}\sqrt{\mathrm{Im}\varepsilon(z,\omega)}$$

$$\boldsymbol{G}^*(z_A,z,\omega)\;C_2(t)\;e^{i(\omega-\omega_0)t} \tag{13}$$

with

$$\Delta_L = \omega_L - \omega_0 \tag{14}$$

Substituting the formal solution of Eq. (13) with the initial condition $C_3(z,\omega,0)=0$

$$C_3(z,\omega,t) = \frac{d_{32}}{\sqrt{\hbar\varepsilon_0\pi}}\,\frac{\omega^2}{c^2}\sqrt{\mathrm{Im}\varepsilon(z,\omega)}$$

$$\boldsymbol{G}^*(z_A,z,\omega)\int_0^t dt'\;C_2(t')\;e^{i(\omega-\omega_0)t'} \tag{15}$$

and that of Eq. (11), with the initial condition $C_1(t=0) = C_1(0)$, into Eq. (12), and employing the integral relation

$$\frac{\omega^2}{c^2}\int dz\varepsilon''(z,\omega)\;G(z_A,z,\omega)G^*(z_A,z,\omega) = \mathrm{Im}\;G(z_A,z_A,\omega) \tag{16}$$

we arrive at

$$\dot{C}_2(t) = i\frac{\Omega_L(t)}{2}e^{-i\vartheta_L}\;e^{-i\Delta_p t}C_1(t) + \int_0^t dt'\;K(t,t')\;C_2(t') \tag{17}$$

with the kernel function at the position z_A

$$K(t,t') = -\frac{|d_{23}|^2}{\hbar\varepsilon_0\pi c^2}\int_0^\infty d\omega\;\omega^2\mathrm{Im}$$

$$\boldsymbol{G}(z_A,z_A,\omega)\;e^{-i(\omega-\omega_0)(t-t')} \tag{18}$$

It is worth noting that all the matter parameters that are relevant for the atomic evolution are contained, via the Green tensor, in the kernel function Eq. (18).

5 Geometric Phase

For a normalized pure state given a with density matrix $\rho(t) = |\psi(t)\rangle\langle\psi(t)|$, the nonadiabatic geometric of quantum evolution of a system between states $|\psi(t)\rangle$ and $|\psi(t')\rangle$ is dened by [31]

$$\Phi_t = \arg\langle\psi(t')|\psi(t)\rangle + i\int_0^t \langle\psi(t')|V^{\dagger}(t)V(t)|(t')\rangle dt, \tag{19}$$

where, $V(t)$ is the time-dependent unitary operator. If that parallel transport $\langle\psi(t')|V^{\dagger}(t)V(t)|(t')\rangle = 0$, the geometric phase is just the total phase

$$\Phi_t = \arg\langle\psi(t')|\psi(t)\rangle, \tag{20}$$

Accordingly, for a pure projectors with $\langle\psi(0)|\psi(t)\rangle \neq 0$, the associated geometric phase is defined as[21]

$$\Phi_t = \arg\langle\psi(0)|\psi(t)\rangle, \tag{21}$$

One may measure Φ_t in interferometry as a relative phase shift in the interference pattern characterized by $\beta e^{i\phi} = \langle\psi(0)|\psi(t)\rangle$, where $\beta = |\langle\psi(0)|\psi(t)\rangle|$ is the visibility [40]. Here, an exact expression of the associated geometric phase can be obtained as

$$\Phi_t = \arg(C_1^*(0)C_1(t) + C_2^*(0)C_2(t)e^{-i\omega_0 t}) = -\arctan\left(\frac{Y(t)}{X(t)}\right), \tag{22}$$

with

$$X(t) + iY(t) = \mathrm{Re}(C_1^*(0)C_1(t) + C_2^*(0)C_2(t)e^{-i\omega_0 t})$$

$$+i\mathrm{Im}(C_1^*(0)C_1(t) + C_2^*(0)C_2(t)e^{-i\omega_0 t}) \tag{23}$$

6 The Reduced Density Operator and Entanglement Measure

A major thrust of current research is to nd an efficient and quantitative measure of entanglement for bipartite system. The concurrence [41,42], negativity, [43] and relative entropy [44] are some of these measures. Also, one of these approaches that based on the eigenvalue spectra of the system density matrices is entropy method [45,46, 47]. Entropy, known as von Neumann entropy [45], is related to the density matrix, which provides a complete statistical description of the system. It is a commonly accepted fact that von Neumann entropy [45] is the unique entanglement measure for bipartite systems in a pure state [48]. From the viewpoint of the Phoenix-Knight [46] entropy formalism, we have investigated the quantum entropy and entanglement of the present system. In order to calculate the entropy $S(t)$, we must obtain the eigenvalues of the reduced density operator. Recalling Eq. (10), the full density matrix $\rho(t) = |(t)\rangle\langle(t)|$, needed for calculating the reduced density matrix $\rho_A(t)$, after the tracing of the reservoir variables, is expressed as

$$\rho_{\mathbf{A}}(t) = \begin{pmatrix} \rho_{11}(t) & \rho_{12}(t) & 0 \\ \rho_{21}(t) & \rho_{22}(t) & 0 \\ 0 & 0 & \rho_{00}(t) \end{pmatrix} \tag{24}$$

where

$$\rho_{11}(t) = |C_1(t)|^2,\ \rho_{12}(t) = C_1(t)C_2^*(t) = \rho_{21}^*(t),\ \rho_{22}(t) = |C_2(t)|^2 \tag{25}$$

and

$$\rho_{00}(t) = \frac{|d_{32}|^2}{\hbar\varepsilon_0\pi c^2}\int_0^{\infty} d\omega\omega^2$$

$$G(z_A, z_A, \omega)\left|\int_0^t dt' C_2(t')e^{(\omega-\omega_0)t'}\right|^2 \tag{26}$$

In deriving $\rho_{00}(t)$, Eq. (26), we have used the integral relation (16). It is apparent that, the nal expression of $\rho_{00}(t)$ depends on the form of the Green tensor $\mathrm{Im}G(z_A, z_A, \omega)$. In terms of the eigenvalues, $chi_y, (y = 1,2,3)$, entropy can be dened as follows [46,49]

$$S(\rho_{\mathbf{A}}) = -\sum_{y=1}^{3} \chi_y \ln \chi_y \tag{27}$$

where $\chi_y, (y = 1,2,3)$ are the roots of the charactersic equation of degree three

$$\chi^3 - [\rho_{11} + \rho_{22} + \rho_{00}]\chi^2 + [\rho_{11}\rho_{22} + \rho_{00}(\rho_{11} + \rho_{22}) - |\rho_{12}|^2]\chi^2$$

$$+(|\rho_{12}|^2\rho_{00} - \rho_{11}\rho_{22}\rho_{00}) = 0 \tag{28}$$

The reduced density matrix is, however, calculated in a general form, hence, entropy of the system can be easily copmuted. The results will depend crucially on the shape of the kernel (18). To gain clearer insight, a comparison between various shapes of the kernel (18) is, however, efficient. This is precisely what is done in the next sections.

7 Applications

7.1 Three-level atom in free space near a perfectly reecting mirror

Besides the free space being interesting in its own right, it will be useful to compare and interpret the outcomes in the following sections. In free space, the excitation spectrum turns into a quasi-discrete set of lines of mid-frequencies k centered about the atomic transition frequency $\omega_k \approx \omega_0 0$. Thus, the Green tensor $G(z_A, z_A, \omega)$, is replaced by the vacuum Green tensor; $G(z_A, z_A, \omega_0)$ [4,5], where

$$\mathrm{Im}G^V(z_A, z_A, \omega_0) = \frac{\omega_0}{6\pi c}\mathbf{I} \tag{29}$$

thus, the kernel Eq. (18) becomes

$$K(t,t') = -\frac{|d_{23}|^2}{\hbar\varepsilon_0\pi c^2}\frac{\omega_0}{6\pi c}\int_0^\infty d\omega_k\,\omega_k^2\,e^{-i(\omega_k-\omega_0)(t-t')} \quad (30)$$

In this case the Weisskopf-Wigner approximation [50] is applied to obtain for $C_2(t)$, Eq. (17),

$$\dot{C}_2(t) = i\frac{\Omega_L}{2}e^{-i\vartheta_L}\,e^{-i\Delta_p t}C_1(t) - \Gamma_0^{32}C_2(t) \quad (31)$$

with the free-space spontaneous emission rate for the transition $|2\rangle \to |3\rangle$

$$\Gamma_0^{32} = \frac{|d_{23}|^2\omega_0^3}{3\hbar\varepsilon_0\pi c^3} \quad (32)$$

It is not difficult to obtain the amplitudes $C_2(t)$ and $C_1(t)$ from equations (11) and (31), using the initial conditions $C_1(t=0) = C_1(0)$ and $C_2(t=0) = C2(0)$, as

$$C_2(t) = \sum_i e^{x_i t}\frac{(x_i+i\Delta_L)C_2(0)+i\frac{\Omega_L}{2}e^{-i\vartheta_L}C_1(0)}{(x_i-x_j)}, \quad i,j=1,2;\ i\neq j \quad (33)$$

$$e^{-i\Delta_L t}C_1(t) = \sum_i e^{x_i t}\frac{[x_i+\Gamma_0^{32}]C_1(0)+i\frac{\Omega_L}{2}e^{i\vartheta_L}C_2(0)}{(x_i-x_j)}, \quad i,j=1,2;\ i\neq j \quad (34)$$

with

$$x_{1,2} = -\frac{\Gamma_0^{32}+i\Delta_L}{2} \pm \frac{1}{2}\sqrt{(\Gamma_0^{32}-i\Delta_L)^2-\Omega_L^2} \quad (35)$$

If the classical pump laser field is resonance with the atomic transition frequency ω_0 ; $\Delta_L = 0$, we have

$$x_{1,2} = -\frac{\Gamma_0^{32}}{2} \pm \frac{1}{2}\sqrt{(\Gamma_0^{32})^2-\Omega_L^2} \quad (36)$$

As we seek for omparison, we will consider the case when $\Omega_L = \Gamma_0^{32}$. In this case the double root are $x_{1,2} = -\Gamma_0^{32}/2$ which yield for the amplitudes $C_2(t)$ and $C_1(t)$ the expressions

$$C_j(t) = e^{-\frac{\Gamma_0^{32}}{2}t}\left[C_j(0)+(-1)^{j+1}\frac{\Gamma_0^{32}}{2}t\left(C_j(0)+(-1)^{j+1}ie^{(-1)^{j+1}h\phi_L}C_k(0)\right)\right],$$

$$j,k=1,2;\quad j\neq k \quad (37)$$

Performing time integral in Eq. (26) with help of Eq. (37), recalling the vacuum Green tensor, Eq. (29), a somewhat lengthy calculations of frequency integral, using the initial condition $C_2(0) = \frac{1}{\sqrt{2}} = C_1(0)e^{i\phi}$, yields

$$\rho_{00}(t) = \left(1-e^{-\Gamma_0^{32}t}\right) - \frac{(\Gamma_0^{32})^2t^2(1+\cos\vartheta)}{2}e^{-\Gamma_0^{32}t} \quad (38)$$

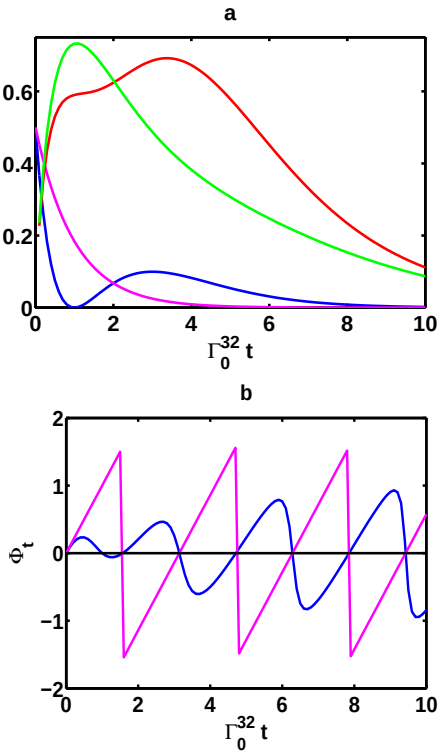

Fig. 1: (a) State $|2\rangle$ Population, $|C2|^2$ [blue, $\vartheta = \pi/2$] and [magenta, $\vartheta = -\pi/2$] and entropy, S [red, $\vartheta = \pi/2$] and [green, $\vartheta = -\pi/2$], (b) the Berry phase t [blue, $\vartheta = \pi/2$] and [magenta, $\vartheta = -\pi/2$], against $\Gamma_{32}t$ for atom in free space with $\Omega_L/\Gamma_{32} = 1$.

With same initial condition in $C_j(t)$ and for $\vartheta = -\pi/2, \pi/2$, the population $|C_2|^2$, entropy, S, and Berry phase, Φ_t, against $\Gamma_{32}t$, are shown in Fig. (1) for an atom in free space. We can see clearly the effect of the damping term, $exp(\Gamma_{32}/2)$, where decay to normal vacuum occurs after few oscillations [51], but with different degrees according to the change in ϑ. Entropy, S, starts with rapid increase - regardless of ϑ value - while it decays to zero slowly or rapidly depending on ϑ sign. For $\vartheta = \pi/2$ all terms in Eq. (23) contribute to Φ_t and the resulting phase exhibits Rabi oscillations with an amplitude increases with time, while for $\vartheta = -\pi/2$, Φ_t reduces to $\Phi_t = \arctan[\cot(\omega_0 t/2)]$ that explains the so tooth evolution of Φ_t with sharp peaks jump to the opposite sign on periods of $\Gamma_{32}t = n\pi/2$; $n = 0,1,2\ldots$. Note, Rabi oscillations are due to the different de-phasing of the off-diagonal coherences caused by environmental inuences [52]. It is worth to note that, because of the very different evolutions of both S and Φ_t, we cannot build any insight about the connection between them. In addition, in free space, as known, we cannot stabilize quantum systems against environmental decoherence and, hence, entanglement revives for short times.

7.2 Three-level atom in placed near a planar dielectric half-space in the weak-coupling regime

Due to the additional noise accompanying absorption, the photonic density of states may be modied, as a result, the integral kernel, Eq. (18), needs to be treated mathematically in a complete dierent way. Taking the time integral of both sides of Eq. (17), it is not difficult to obtain

$$C_2(t) = C_2(0) + \frac{i\Omega_L}{2} e^{-i\vartheta_L} \int_0^t dt'\, e^{-i\Delta_L t'} C_1(t') + \int_0^t dt'\, \mathscr{K}(t,t')\, C_2(t') \tag{39}$$

with

$$\mathscr{K}(t,t') = \frac{|d_{23}|^2}{\hbar\varepsilon_0\pi} \int_0^\infty d\omega \frac{\omega^2}{c^2} \mathrm{Im}\, \boldsymbol{G}(z_A, z_A, \omega) \frac{e^{-i(\omega-\omega_0)(t-t')} - 1}{i(\omega-\omega_0)} \tag{40}$$

For an atom located in free-space near a dielectric, the Green tensor for the system can be divided into two parts [3], i. e., the vacuum Green tensor given by Eq.(29), $G^V(z_A, z_A, \omega)$, and the Green tensor, $G^R(z_A, z_A, \omega)$, that describes the effect of reflection at the surface of discontinuouty of the body, thus

$$G(z_A, z_A, \omega) = G^R(z_A, z_A, \omega) + G^V(z_A, z_A, \omega) \tag{41}$$

In the weak-coupling regime, Markov approximation can be safely applied because of ignoring the memory effects. This assumption implies that

$$\frac{e^{i(\omega_0-\omega)(t-t')} - 1}{i(\omega_0-\omega)} \to \pi\delta(\omega_0-\omega) + i\mathscr{P}\frac{1}{\omega_0-\omega} \tag{42}$$

thus

$$\mathscr{K}(t,t') = -\Gamma^{32}/2 + i\delta\omega_0 \tag{43}$$

where the modied, by the presence of the body, decay rate Γ^{32} and the level shift $\delta\omega_0$, are respectively,

$$\Gamma^{32} = \Gamma_0^{32} + \frac{2|d_{23}|^2}{\hbar\varepsilon_0} \frac{\omega_0^2}{c^2} \mathrm{Im}\, G^R(z_A, z_A, \omega_0) \tag{44}$$

$$\delta\omega_0 = \frac{|d_{23}|^2}{\hbar\varepsilon_0\pi} \mathscr{P} \int_0^\infty d\omega \frac{\omega^2}{\omega_0^2} \frac{\mathrm{Im}\, G^R(z_A, z_A, \omega)}{(\omega-\omega_0)} \tag{45}$$

Obviousely, in contrast to free space, the vacuum uctuations felt by an atom are inhomogeneously and anisotropically changed by the presence of the bodies. Following the approach of Dung et al., [4], and after Recalling the Kramers-Kronig relation [3] for the Green tensor, we may approximately rewrite $\delta\omega_0$ as

$$\delta\omega_0 = \frac{|d_{23}|^2\omega_0^2}{\hbar\varepsilon_0 c^2} \mathrm{Re}\, G^R(z_A, z_A, \omega_0) - \frac{|d_{23}|^2}{\pi} \int_0^\infty d\omega \frac{\omega^2}{\omega_0^2} \frac{\mathrm{Im}\, G^R(z_A, z_A, \omega)}{(\omega+\omega_0)} \tag{46}$$

where the second term can be ignored as it is weakly sensitive to the atomic transition frequency and small compared to the rst one. Substituting (43) into (39) and taking the time derivative of both sides with the setting of $\Gamma_{32}/2 = \varpi_{32}$, for simplicity, we obtain

$$\dot{C}_2(t) = i\frac{\Omega_L(t)}{2} e^{-i\vartheta_L}\, e^{-i\Delta_L t} C_1(t) + (-\varpi^{32} + i\delta\omega_0)\, C_2(t) \tag{47}$$

Following the same procedure as in the previous section, the amplitudes $C_1(t)$ and $C_2(t)$ can be obtained as

$$e^{-i\Delta_p t} C_1(t) = \sum_i e^{y_i t} \frac{[y_i - (-\varpi^{32} + i\delta\omega_0)] C_1(0) + i\frac{\Omega_L}{2} e^{i\vartheta_L} C_2(0)}{(y_i - y_j)}, \tag{48}$$

$$C_2(t) = \sum_i e^{y_i t} \frac{(y_i + i\Delta_L) C_2(0) + i\frac{\Omega_L}{2} e^{-i\vartheta_L} C_1(0)}{(y_i - y_j)}, \quad i,j = 1,2, \quad i \neq j \tag{49}$$

and, due to the unite trace,

$$\rho_{00}(t) = 1 - |C_1(t)|^2 - |C_2(t)|^2 \tag{50}$$

where

$$y_{1,2} = -\frac{(\varpi^{32} - i\delta\omega_0) + i\Delta_l}{2} \pm \sqrt{[(\varpi^{32} - i\delta\omega_0) - i\Delta_l]^2 - \Omega_l} \tag{51}$$

7.3 Model permittivity of Drude-Lorentz type

We consider two innite half-space dielectric medium [3] such that

$$\varepsilon(\mathbf{r}, \omega) = \begin{cases} \varepsilon(\omega) & \text{if } z \leq 0 \\ 1 & \text{if } z > 0 \end{cases} \tag{52}$$

To give an impression of what can be observed in real situation, let choose a planar dielectric surface of permittivity modeled by the widely-used-in-practice Lorentz type as [53]

$$\varepsilon(\omega) = 1 + \frac{\omega_p^2}{\omega_T^2 - \omega^2 - i\omega\gamma} \tag{53}$$

where ω_T and γ are the medium oscillation frequencies and linewidths, respectively, and ω_p correspond to the coupling constants. For $z > 0$, but small compared with the wave length, $kz \ll 1$, using the results obtained by Scheel et al. [54] of the reflection part of the Green tensor yields for the decay rate

$$\Gamma^{32} \approx \frac{3\Gamma_0^{32}}{8} \left(1 + \frac{d_z^2}{d^2}\right) \left(\frac{c}{\omega_0 z}\right)^3 \frac{\varepsilon_I(\omega_0)}{|\varepsilon(\omega_0)+1|^2} \tag{54}$$

Similarly, the line shift reads

$$\delta\omega_0 = \frac{3\Gamma_0^{32}}{32}\left(1+\frac{d_z^2}{d^2}\right)\left(\frac{c}{\omega_0 z}\right)^3 \frac{|\varepsilon(\omega_0)|^2-1}{|\varepsilon(\omega_0)+1|^2} \tag{55}$$

It has been shown [55] that despite being the phase gained by a joint state, its value is fundamentally dependent on the harmonic oscillator nature of the vibrational mode. Because of the intra-subsystem coupling, the evolution of the system can be very different from the free space case. Moreover, considering the Drude-Lorentz model stimulates important observations such that the exhibition of a band gab between the transverse frequency ω_T and longitudinal frequency $\omega_G = \sqrt{\omega_T^2+\omega_p^2}$ and incorporation of surface-guided-waves [4].

Such an effct can give rise to strong collective effects, which are necessarily required to generate substantial entanglement [39]. Inside the band gap most of the energy emitted by the atom is absorbed by the medium in the course of time, namely, non-radiative decay dominates. It worth to note that, when the band gap is smoothed, this means that the fraction of light that escapes to free space can increase, specially with increasing value of γ/ω_T, this is simply clear from Fig. (15a), and thus radiative decay dominates [4]. Note, inside the band gap $\delta\omega_0$ changes its sign as Γ_{32} decreases from its maximum as possible, so, its contribution to interaction becomes weak and can be ignored. These facts together give rise to approximate the complex amplitudes $C_m(t), m = 1,2$, Eqs. (48, 49) to be, on setting $\Delta_L = 0$, the same form as Eqs. (37) of free space with the replacement of the free space decay rate Γ^{32} by ϖ^{32}. We expect a similar behavior as in free space but with longer time scale due to the effct of the body expressed in the dependence of Γ^{32} on the dielectric parameters, as seen from comparison of Figs. 1, 2 and 3. When we extend the discussion to include a wider range of the frequency γ/ω_T, namely, below, above and in the band gap, it will be interesting to include the level shift in our treatment. We used the same set of parameters to picture the numerical results as mesh plots in Figs. (4-6) where the linewidth changes as $\gamma/\omega_T = 0.001, 0.01$ and 0.1, while a cross section from the mesh plots are given in Fig. 7. Figures show that a similar behavior of both $|C_2|^2$ and Φ_t, while an opposite development of S is noticed. In the the absorption band region where $\omega_G \in [\omega_T, 1.12\omega_T]$, regardles of the time scale, both $|C_2|^2$ and S amplitudes damped to zero and the atom and eld are in separable state while neighboring the band gap, the atom and the fields are strongly correlated. The phase Φ_t reaches its negative maximum . Below the band gap, as time passes, $|C_2|^2$ decreases slowly, while, on increasing γ/ω_T, $|C_2|^2$ shows rapid increase. An opposite behavior is noticed for entropy S below the band gap but for not high broadened linewidth, see Fig. (6). Below and above the band gap, Φ_t

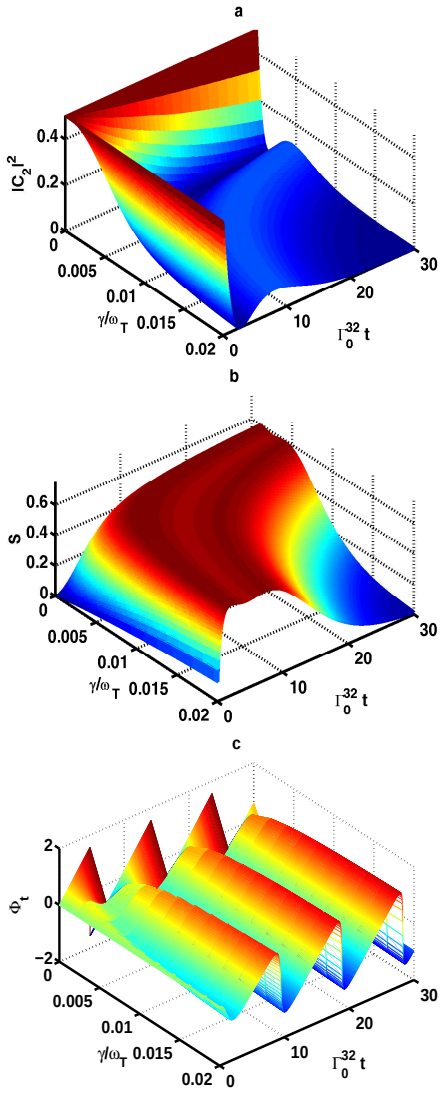

Fig. 2: Mesh plot of $|C_2|^2$ (a), entropy, S (b), and Berry phase Φ_t (c), as functions of the bandwidth γ/ω_T and $\Gamma_0^{32}t$ near a planar dielectric half-space, with $\Omega_L = \varpi^{32}, \omega_0 = 1.12\omega_T, \omega_p = 0.5\omega_T$, $z = 0.05\lambda_T$ for $\vartheta = \pi/2$.

exhibits opposite sharp peaks of maximum unity disappear by increasing γ/ω_T. Here, the resulting total phase t written as a function of its maximum and minimum of the amplitudes, influences the initial system state $|\psi(0)\rangle = |a\rangle_{at}|\{0\}\rangle_f$ to evolve antisymmetrically as $|a\rangle_{at}|\{0\}\rangle_f \rightarrow \frac{1}{2}(|a\rangle_{at}|\{0\}\rangle_f - i\sqrt{3}|c\rangle_{at}|1\rangle_f) \rightarrow \frac{1}{2}|a\rangle_{at}(|\{0\}\rangle_f - i\sqrt{3}|1\rangle_f)$, where $|a\rangle_{at} = \frac{1}{\sqrt{2}}(|1\rangle + |2\rangle)$ and $|c\rangle_{at} = \frac{1}{\sqrt{2}}(|3\rangle + |2\rangle)$. This can be interpreted as follows: If the initial state is taken to be $|a\rangle_{at}|\{0\}\rangle_f$, we can write,

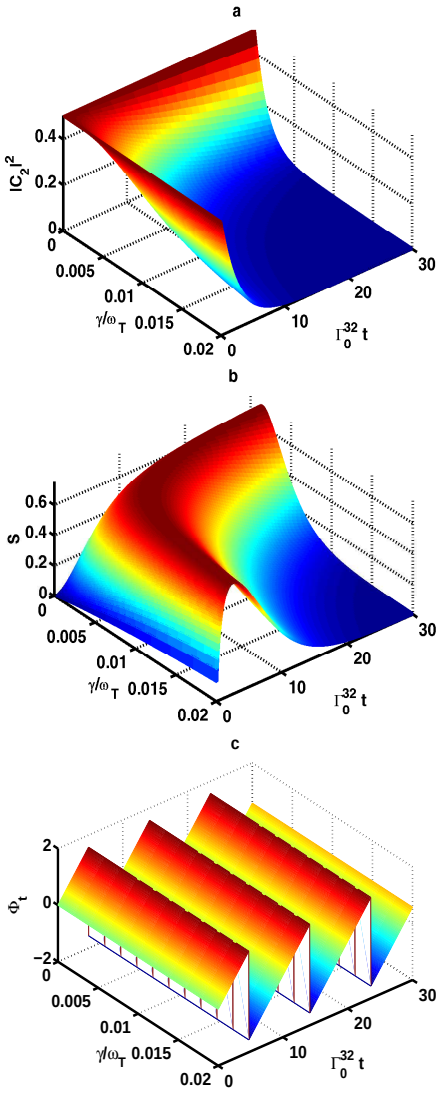

Fig. 3: The same as Fig. 2 but for $\vartheta = -\pi/2$

$$|a\rangle_{at}|\{0\}\rangle_f = \cos\left(\int_0^t dt'\Phi_t(t')\right)|a\rangle_{at}|\{0\}\rangle_f$$

$$-i\sin\left(\int_0^t dt'\Phi_t(t')\right)|c\rangle_{at}|1\rangle_f \qquad (56)$$

If we consider, $\Phi_t(t') = \Phi_t$, then for $t\Phi_t = \pi/3$, previous results can be easily reached, which demonstrates that the wave function behind the system acts as $\cong 35\% : 65\%$ beam splitter (BS) with Bell angle controls degree of superpostion of photon states $|\{0\}\rangle_f$ and $|1\rangle_f$. We, however, have could generate a degree of entanglement between input and output photons, a very important question needs to be answered, that is, why the atom and the eld remain in separable state above the band gap? The answer is as follows: any value of the Bell angle t that reects the degree of entanglement between input and output photons except for $\Phi_t = 0$ or $\pm\pi$, means partial overlap between the initial and final wave functions of the system, i. e., noncyclic evolution.

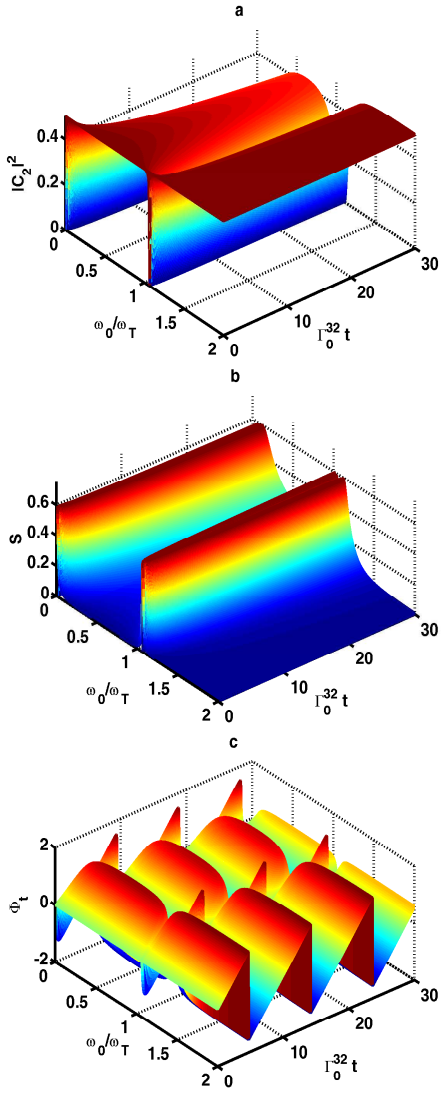

Fig. 4: Mesh plot of $|C_2|^2$ (a), entropy, S (b), and Berry phase Φ_t (c), against ω_0/ω_T and $\Gamma^{32}t$ near a planar dielectric half-space, with $\Omega_L = \varpi^{32}, \omega_p = 0.5\omega_T, z = 0.05\lambda_T$ for $\gamma = 10^{-3}\omega_T$.

Hence, destructive interference is more pronounced. As a consequence, Entropy S partially vanishes, see Figs. (4, 5 and 7). A full cyclic evolution with long-lived entanglement can be noticed below the band gap in Fig. (10). It is worth mentioning that below the band gap and at the eld resonance $(\omega_0 \approx \omega_T)$ frequencies, a photon emitted at such a frequency is typically captured by the surface for some time, i.e., a photon absorption dominates

[4], and hence, no interference effects could modify the phase angle of the emitted photons as long as γ/ω_T preserved small, see Figs. (4b and 7b). In the low-frequency region $(\omega_0 < \omega_T)$, where surface-guided waves are typically excited, radiative decay dominates, i.e., the probability of a photon being absorbed is also small, and hence, interference effects become more effective. This clarifies why by increasing the damping parameter, γ/ω_T, the angle between the initial and final photon states reduced remarkably to be no longer approaches π, see Fig. 7c, and explains why atom-eld entanglement below band gap is more pronounced, see Fig. (7b).

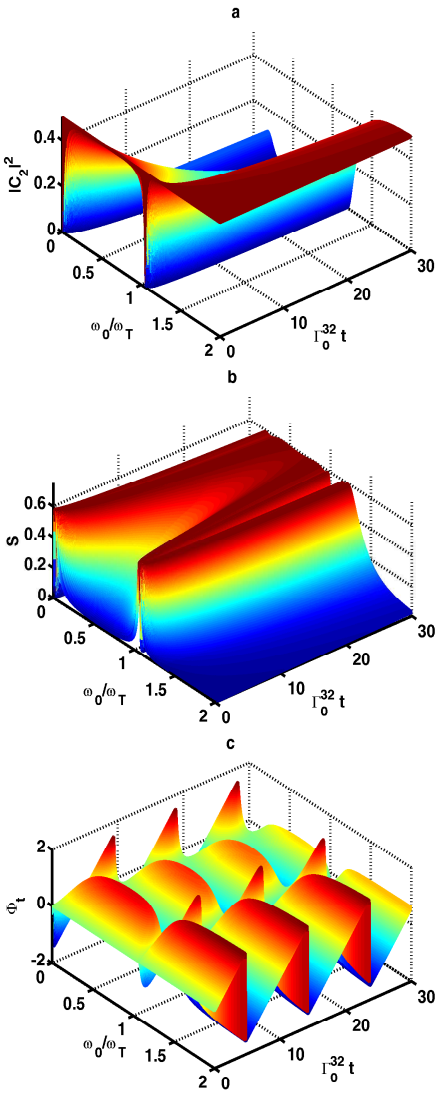

Fig. 5: The same as Fig. 4 but for $\gamma = 10^{-2}\omega_T$.

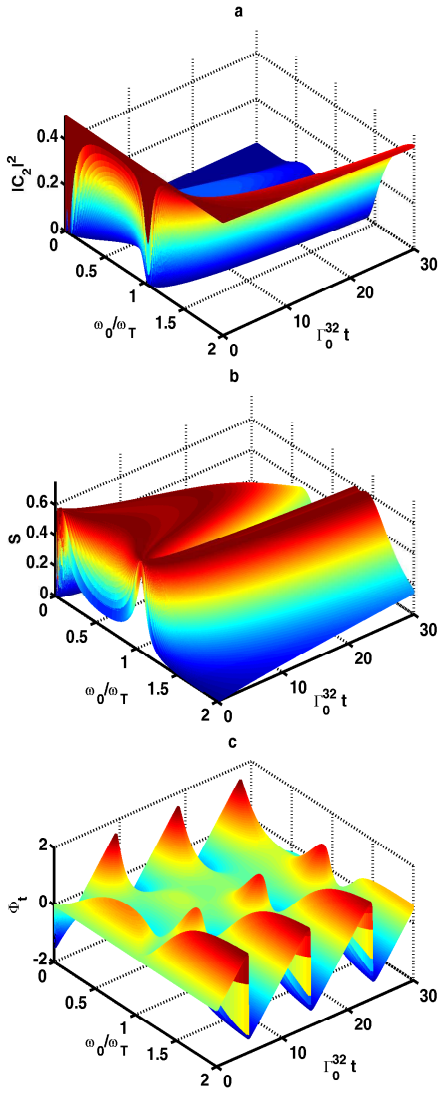

Fig. 6: The same as Fig. 4 but for $\gamma = 10^{-1}\omega_T$

Figures 8-11 illustrate the dependence of $|C_2|^2$, Φ_t, and S on line shift $\delta\omega_0$ as well as the decay rate Γ^{32} with various values of the bandwidth parameter γ. The figures reveal that with the decrease of γ/ω_T, rapid Rabi oscillations are created, specially far below the band gap; $\omega_0 \ll \omega_T$, where, oscillations strongly overlap during all time stages, due to the rapid energy transfer between the atom and the medium to the extent that the populations of the levels $|1\rangle$ and $|2\rangle$ overlap except for small course of time. In this case, the initial state $|a\rangle_{at}|\{0\}\rangle_f$ evolves eventually between symmetricall and antisymmetricall states as $|a\rangle_{at}|\{0\}\rangle_f \rightarrow \frac{1}{2}|a\rangle_{at}(|\{0\}\rangle_f \pm i\sqrt{3}|1\rangle)$, thus, a 35% : 65% BS is clearly noticed. An important observation is that, for short time scale in the low-frequency region $(\omega_0 < \omega_T)$, as possible as γ/ω_T is preserved small, the population, exhibits water waves evolution, that seems clearly as an envelope of Φ_t Rabi

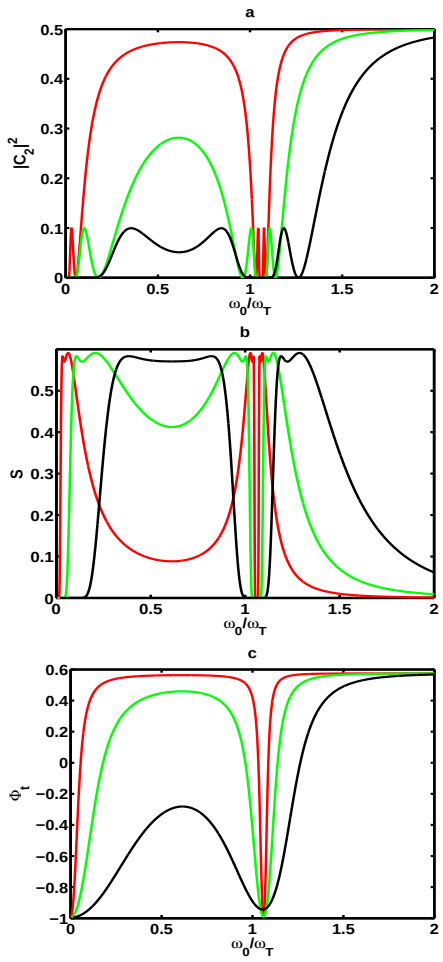

Fig. 7: Cross section depicted for $|C_2|^2$ (a), entropy, S (b), and Berry phase Φ_t (c), against ω_0/ω_T when $\Gamma_0^{32}t = 10.0$ and $z = 0.05\lambda_T$, where, red, green and black lines are for $\gamma = 10^{-3}\omega_T, \gamma = 10^{-2}\omega_T$ and $\gamma = 10^{-1}\omega_T$, respectively.

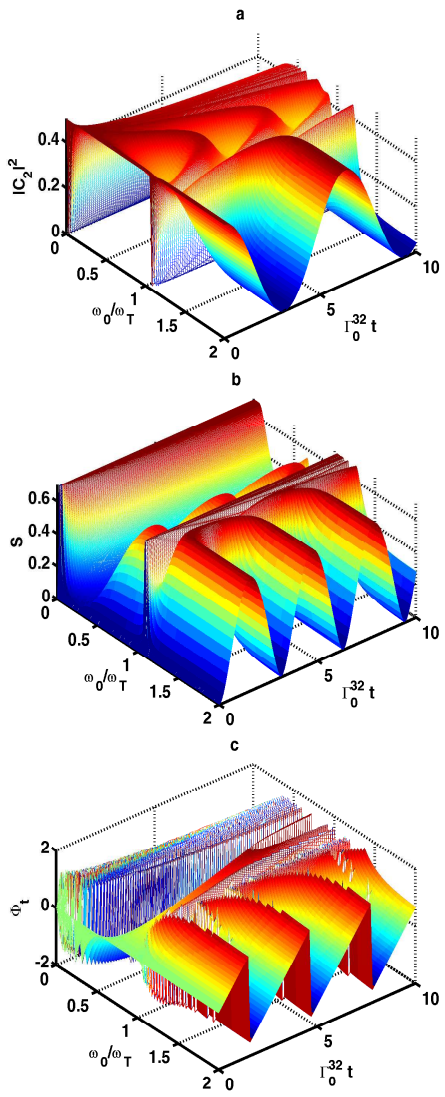

Fig. 8: The same as Fig. 4 but when taking into account the effect of both Γ^{32} and $\delta\omega_0$

oscillations. It is worth noting that, for Φ_t, a similar behavior has been noticed for a Λ-type three level atom interacts with single mode in the presence of one-dimensional photonic band gap [20]. In such a region, separable atom-field states are clearly produced. On increasing γ/ω_T and as time passes, Φ_t gradually vanishes till disappears completely except for slightly small region, which resluted in a long-lived atom-field entanglement extended over all below band gap region, compare Figs. (8) and (10), also, Figs. (11b) and (11c). In this case, a full cyclic wave evolution is produced, where the initial state $|a\rangle_{at}|\{0\}\rangle_f$ evolves symmetrically as $|a\rangle_{at}|\{0\}\rangle_f \rightarrow \frac{1}{2}|a\rangle_{at}(|\{0\}+|1\rangle)$, thus, a 50% : 50% BS is clearly noticed.

The effect of the distance z_A of the atom from the plate surface supports our previous analysis. Note, the term $(\approx z_A^{-3})$ in Eqs. (54) and (55), which is proportional to $\varepsilon_I(\omega_0)$, is closely related to the virtual photon emission with subsequent medium quasiparticle excitation (nonradiative decay), i.e., energy transfer from the atom to the medium. Thus, we expect to achieve our goal more simply. In Figs. (12-15), $|C_2|^2$, S, and Φ_t have been pictured against ω_0/ω_T and z_A/λ_T for different values of γ/ω_T. One can easily realize that Φ_t undergoes fast Rabi oscillations as long as the atom jumps to state $|2\rangle$. Moreover, one can easily notice that $|C_2|^2$ represents a 3D envelop of Φ_t in the upper half plane while similar behavior to Φ_t is notice for entropy S. Above band gap, Rabi oscillations disappear where a kind of steady entanglement appears extended over all above band gap region. In the corresponding region Φ_t has fixed values regardless of the distant of the atom from the medium. Those figures shape is preserved even if γ/ω_T increses

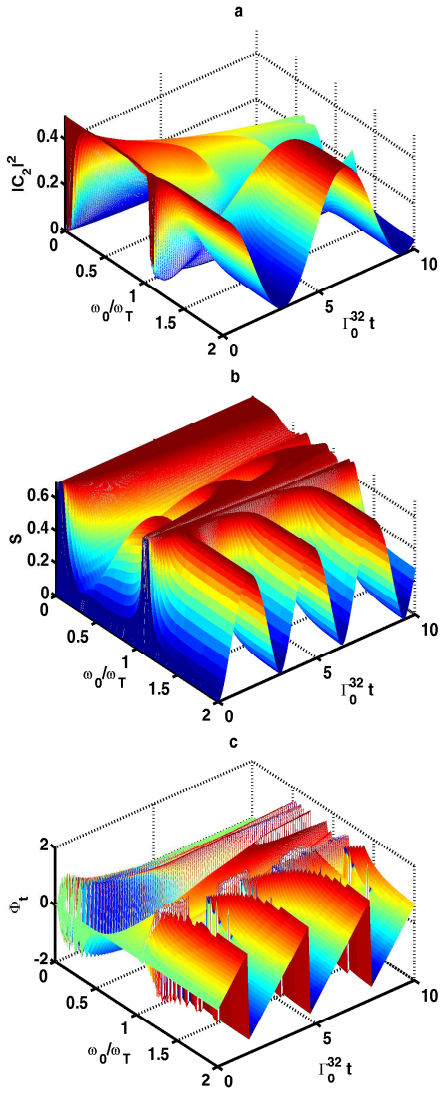

Fig. 9: The same as Fig. 8 but for $\gamma = 10^{-2}\omega_T$

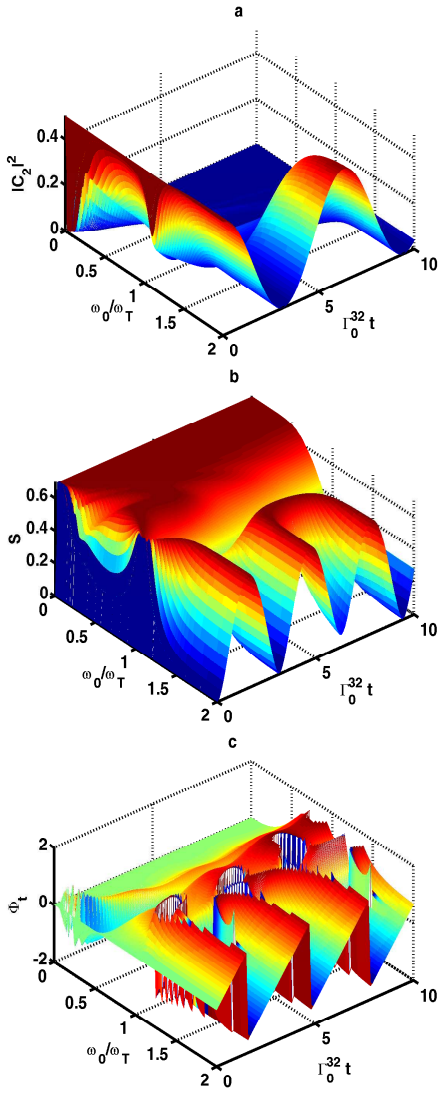

Fig. 10: The same as Fig. 8 but for $\gamma = 10^{-1}\omega_T$

except for extending of the steady entanglement region below and above band gap, see Figs. (13, 14). Hwoever, it is clear that, depending on whether Φ_t vanishes or not, we can distinguish easily where the atom-cavity system is entangled or separable with support of Figs. (13b,c, 14b,c and 15b,c).

Moreover, such interaction setting up is potentially interesting for its ability to process information in a novel way and might nd application in models of quantum logic gates. In fact, in quantum computation, operations are performed by means of single-qubit and multiple-qubit quantum logic gates [56]. One could use the present model, acting as BS, to generate a C-NOT gate, i.e., universal quantum logic gate based on three-level atom. In a single photon Mach-Zhender (M-Z) interferometer [57], which provides two possible paths for a single photon input to be transmitted to the output, for an equal path lengths, $|a\rangle_{at}|\{0\}\rangle_f \rightarrow |a\rangle_{at}(|\{0\}\rangle_f \pm |1\rangle_f)$, our system can be a suitable device so that a photon input will be counted with certainty at the detector by controlling the adjustable parameters. However, for unequal paths, $|a\rangle_{at}|\{0\}\rangle_f \rightarrow \frac{1}{2}|a\rangle_{at}(|\{0\}\rangle_f \pm i\sqrt{3}|1\rangle_f)$, we can insert a phase shift devices into either path and thus change the interference conditions [57]. In this case, an additional polarising beam splitter (PBS) is effective, where, for an emitted photons, PBS redirects vertically polarized photons (say in state $|V\rangle$) without affecting horizontally polarized photons (say in state $|H\rangle$) such that a C-NOT gate can be obtained as

$$\alpha|H\rangle_1 + \beta|V\rangle_2 \rightarrow \alpha|H\rangle_{1'} + \beta|V\rangle_{2'} \qquad (57)$$

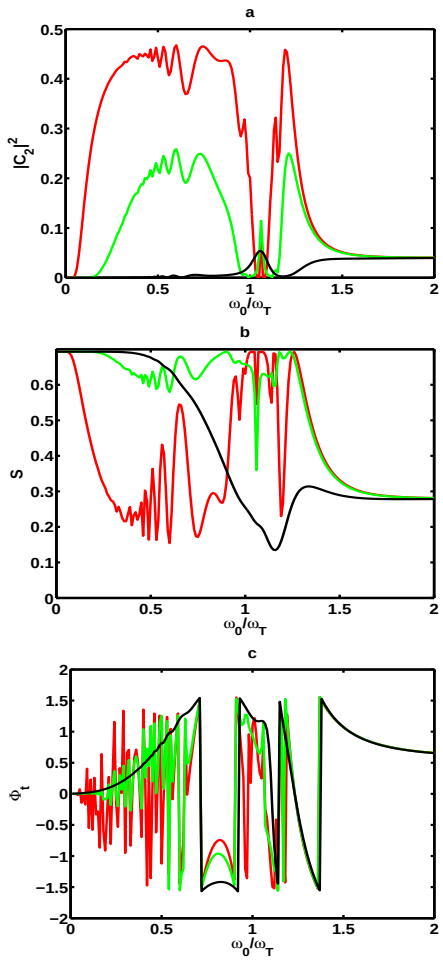

Fig. 11: The same as Fig. 7 but when taking into account the effect of both Γ^{32} and $\delta\omega_0$

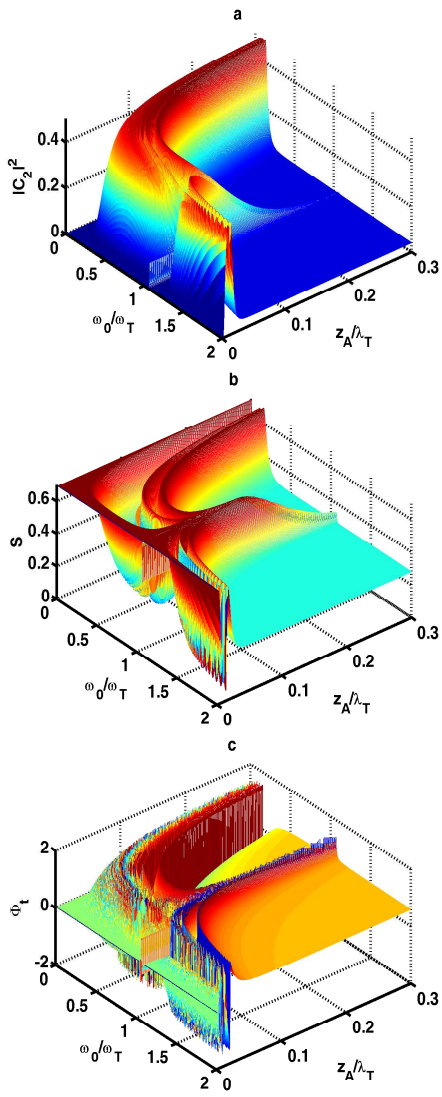

Fig. 12: Mesh plot of $|C_2|^2$ (a), entropy, S (b), and Berry phase Φ_t (c), against ω_0/ω_T and z_A/λ_T near a planar dielectric half-space when $\Gamma^{32}t = 2$ and $\omega_p = 0.5\omega_T$ for $\gamma = 10^{-3}\omega_T$

8 Summary and Conclusions

Based on the analysis above, our study may be considered as a multi-functional. Under the influence of neighboring dielectric, a system of an interacting three-level atom and vacuum electromagnetic field, evolve as an effective entangled two-qubit system, acts as beam splitter (BS) as well as a tool used for testing photon-photon entanglement and looking for an optimized connection between atom-field entanglement and Berry phase to be used as a typical entanglement probe.

To be quite general, we first presented a solution for wave function, without specifying the dielectric properties used in the neighborhood of the atom-field interaction.

During study, the medium oscillation frequency, ω_T , atomic transition frequency, ω_0 , distance of the atom from the dielectric surface, z_A/λ_T and Rabi strength of the driving classical, Ω_L as well as its phase ω_L , are considered as our effective tools. We show that, adjusting the Bell angle settings between the input and output photon to symmetrically or antisymmetrically, we can build a principal signature of strong atom-cavity correlation. To achieve this goal, two essential scenarios can be applied:

–For fixed position of the atom from the medium, utilizing a medium of suitable oscillation frequency ω_T, a correct resonant atomic transition frequency can be produced, hence, a cyclic wave evolution can be generated, i.e, in-phase entangled photon evolution,

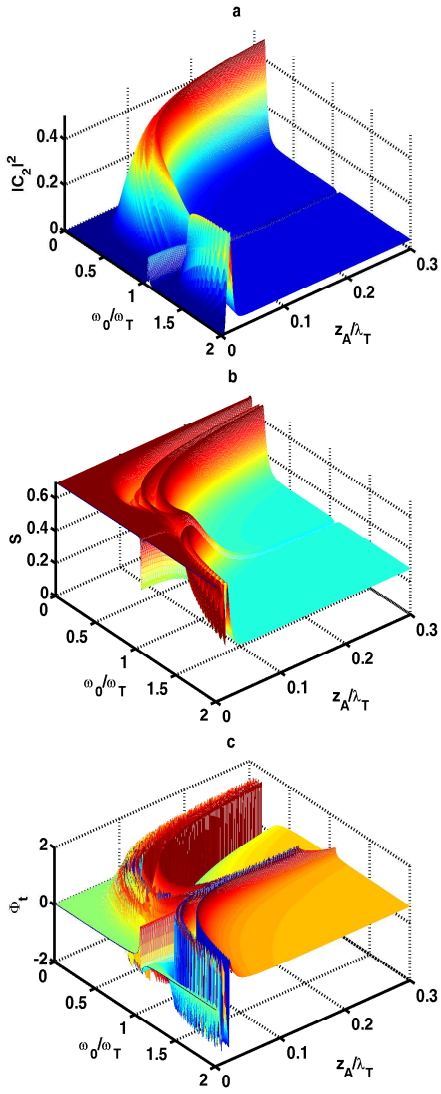

Fig. 13: The same as Fig. 12 but for $\gamma = 10^{-2}\omega_T$

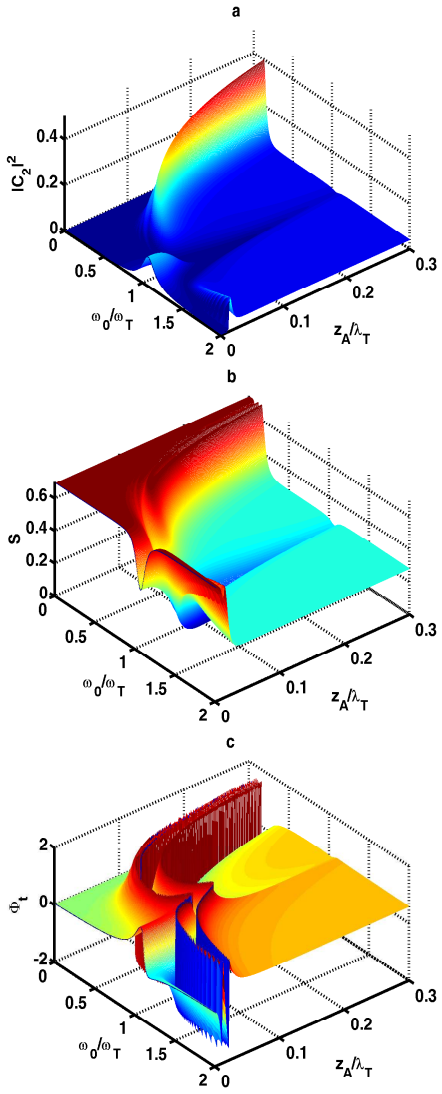

Fig. 14: The same as Fig. 12 but for $\gamma = 10^{-1}\omega_T$

specially with increased medium oscillation linewidth γ, below and neighboring band gap, which resulted in a strong atom-cavity entanglement can survive longer than the corresponding in free space.

–For variant distance from the medium, atom-cavity entanglement become more efficient. In this case, for a distance $z_A \leq \lambda_T$, entanglement extended over wide range of the ratio between the atomic transition frequency and medium oscillation frequency, ω_0/ω_T, namely, below, above and in the band gap region.

References

[1] E. M. Purcell, Phys. Rev., **69**, 681, (1946).
[2] M. Lewenstein, T. W. Mossberg and R. J. Glauber, Phys. Rev. Lett., **59**, 775 (1987).
[3] W. Vogel and D.-G. Welsch, Quantum Optics, 3rd edition.(WILEY-VCH Verlag GmbH & Co. KGaA, Weinheim), (2006).
[4] H. T. Dung, L. Knöll and D.-G. Welsch, Phys. Rev., **A 64**, 013804, (2001); H. T. Dung, L. Knöll and D.-G. Welsch,Phys. Rev., **A 62**, 053804 (2000).
[5] L. Knöll, S. Scheel, and D.-G. Welsch, In Coherence and Statistics of Photons and Atoms, edited by J. Peřina (Wiley, New York), (2001).
[6] I. V. Bondarev and Ph. Lambin, Phys. Rev., **B 70**, 035407 (2004).
[7] J. R. Buck and H. J. Kimble, Phys. Rev., **A 67**, 033806 (2003).

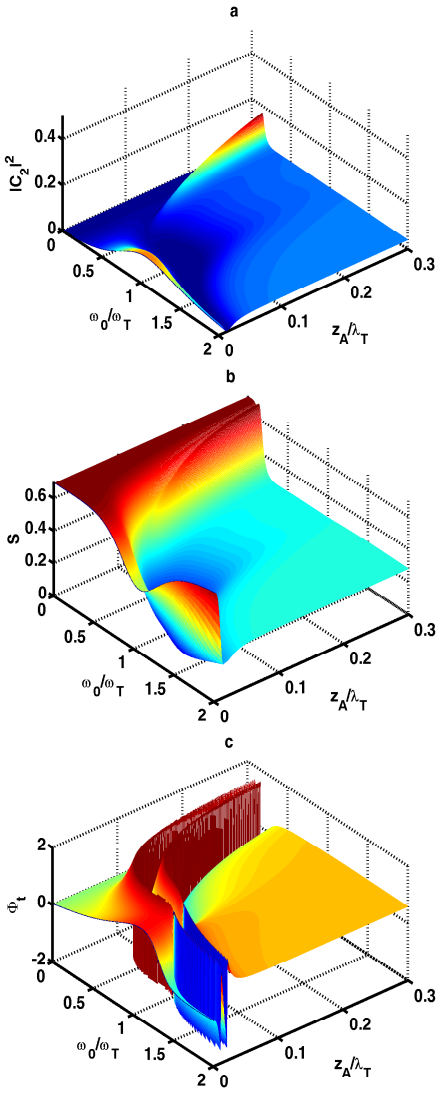

Fig. 15: The same as Fig. 12 but for $\gamma = 5 \times 10^{-1} \omega_T$

[8] V. V. Klimov and M. Ducloy, Phys. Rev., **A 69**, 013812 (2004).
[9] M. Florescu and S. John, Phys. Rev., **A 64**, 033801 (2001).
[10] M. Sugawara, Phys. Rev., **B 51**, 10743 (1995).
[11] E. Schrödinger, Naturwissenschaften, **23**, 807, 823, 844 (1935); A. Einstein, B. Podolsky, and N. Rosen, Phys. Rev., **47**, 777 (1935); R. Horodecki, P. Horodecki, M. Horodecki and K. Horodecki, Rev. Mod. Phys., **81**, 865 (2009).
[12] M. A. Nielsen and I. L. Chuang, Quantum Computation and Quantum Information, (Cambridge University Press, Cambridge, UK), (2000).
[13] A. K. Ekert and S. J. D. Phoenix, J. Mod. Opt., **38**, 19 (1991).
[14] L. Hartmann , W. Dür and H.-J. Briegel, New J. Phys., **9**, 230 (2007).
[15] C. E. López, G. Romero and J. C. Retamal, eprint: arXiv:quant-ph/1007.1951v1, (2010).
[16] J. Suzuki, C. Miniatura, and K. Nemoto1, eprint: arXiv:quant-ph/1002.4716v2, (2010).
[17] E. Agudelo, B. A. Rodriguez, K. M. Fonseca-Romero, eprint: arXiv:quant-ph/1002.4242v1, (2010).
[18] A. M. Basharov, JETP Lett., **75**, 123 (2002); Z. Ficek and R. Tanaś, J. Mod. Opt., **50**, 2765 (2003).
[19] H. T. Cui, L. C. Wang, and X. X. Yi, Eur. Phys. J., **D 41**, 385 (2007).
[20] M. Abdel-Aty, Appl. Phys., **B 88**, 29 (2007).
[21] N. Sandhya and S. Banerjee, eprint: arXiv:quant-ph/1103.2587v1, (2011)
[22] B. Basu, Europhys. Lett., **73**, 833 (2006).
[23] E. Sjöqvist, Phys. Rev., **A 62**, 022109 (2000).
[24] B. Hessmo and E. Sjöqvist, Phys. Rev., **A 62**, 062301 (2000); M. Ericsson et al., Phys. Rev. Lett., **91**, 090405 (2003).
[25] D. M. Tong, E. Sjöqvist, L. C. Kwek, C. H. Oh, M. Ericsson, Phys. Rev., **A 68**, 022106 (2003).
[26] Pétér Lévay, J. Phys. A: Math. Gen., **37**, 1821 (2004).
[27] V. Vedral, Int. J. Quantum Inf., **1**, 1 (2003); M. Ericsson, E. Sjöqvist, J. Brännlund, D.K.L. Oi, A.K. Pati, Phys. Rev., **A 67**, 020101(R) (2003); A. Carollo, I. Fuentes-Guridi, M.F. Santos, V. Vedral, Phys. Rev. Lett., **92**, 020402 (2004).
[28] J. J. Garcia-Ripoll, J. I. Cirac Phys. Rev. Lett., **90**, 127902 (2003); S. L. Zhu, Z.D. Wang Phys. Rev. Lett., **91**, 187902 (2003); J. A. Jones, V. Vedral, A. Ekert, and G. Castagnoli, Nature, **403**, 869 (2000); E. Knill, Nature, **434**, 39 (2005).
[29] X. D. Zhang, S. L. Zhu, L. Hu, Z. D. Wang, Phys. Rev., **A 71**, 014302 (2005); Z. S. Wang, C.F. Wu, X. L. Feng, L. C. Kwek, C. H. Lai, C. H. Oh, V. Vedral, Phys. Rev., **A 76**, 044303, (2007).
[30] S. Pancharatnam, Proc. Indian Acad. Sci., **A 44**, 247 (1956).
[31] M. V. Berry, Proc. R. Soc. London Ser., **A 392**, 45 (1984).
[32] Y. Aharonov and J. S. Anandan, Phys. Rev. Lett., **58**, 1593 (1987)
[33] J. Samuel and R. Bhandari, Phys. Rev. Lett., **60**, 2339 (1988).
[34] D. M. Tong, E. Sjöqvist, S. Filipp, L. C. Kwek, C. H. Oh, Phys. Rev., **A 71**, 032106, (2005); Y. Ben-Aryeh, J. Opt., **B 6**, R1 (2004); A. Bohm, A. Mostafazadeh, H. Koizumi, Q. Niu and J. Zwanziger, J. Phys. A: Math. Theor., **43**, (2010).
[35] L. -A. Wu, P. Zanardi, and D. A. Lidar, Phys. Rev. Lett., **95**, 130501 (2005).
[36] I. Fuentes-Guridi, A. Carollo, S. Bose, and V. Vedral, Phys. Rev. Lett., **89**, 220404 (2002).
[37] X. X. Yi, L. C. Wang, and T. Y. Zheng, Phys. Rev. Lett., **92**, 150406, (2004).
[38] C.-Y. Chen, S. Kang and M. Fenbg, Int. J. Theor. Phys., **48**, 2928, (2009).
[39] Ö. Cakir, H. T. Dung, L. Knöll and D.-G. Welsch, Phys. Rev, **A 71**, 032326 (2005).
[40] E. Sjöqvist, Phys. Lett., **A 286**, 4 (2001).
[41] W. K. Wootters, Phys. Rev. Lett., **80**, 2245 (1998).
[42] H. Xiang, S. Jin-Qiao, S. Jian and Z. Shi-Qun, Commun. Theor. Phys., **57**, 29 (2012).
[43] G. Vidal and R.F. Werne, Phys. Rev., **A65**, 032314 (2002).
[44] V. Vedral and M.B. Plenio, Phys. Rev., **A57**, 1619 (1998) .
[45] J. von Neumann, Götingger Nachr., **273**, (1927).
[46] S. J. D. Phoenix, P. L. Knight, Phys. Rev., **A44**, 6023 (1991); Phys. Rev. Lett., **66**, fg.2033 (1991).

[47] M. S. Ateto, Int. J. Theo. Phys., **49**, 276 (2010).
[48] S. Popescu, Phys. Rev. Lett., **72**, 797 (1994).
[49] V. Vedral, M. B. Plenio, M. A. Rippin and P. L. Knoght, Phys. Rev. Lett., **78**, 2275 (1997).
[50] M. O.Scully and M. S. Zubairy, Quantum Optics, 1st edition. (Cambridge University Press), (1997)
[51] M. Woldeyohannes and S. John, J. Opt. B: Quantum Semiclass. Opt., **5**, R43, (2003).
[52] D. F. Walls, and G . J . Milburn, Phys. Rev. A31, 2403 (1985); S. J. D. Phonix, Phys. Rev., **A41**, 5132 (1990).
[53] [52] Ho Trung Dung, S. Y. Buhmann, L. Knöll, D.-G. Welsch, S. Scheel and J. Kästel, Phys. Rev., **A 68**, 043816 (2003).
[54] S. Sheel, L. Knöll, and D.-G. Welsch, Acta. Rhys. Slov., **49**, 585 (1999c).
[55] A. Ekert, R. Jozsa, Rev. Mod. Phys., **68**, 733 (1996); I. Funetes-Guridi, S. Bose, V. Vedral, Phys. Rev. Lett., **85**, 5018, (2000).
[56] D. Bouwmeester, A. Ekert, A. Zeilinger, The Physics of Quantum Information (Springer, Berlin Heidelberg New York), (2001); G. Leuchs, T. Beth, Quantum Information Processing (Wiley-VCH, Weinheim), (2003).
[57] D. F. Walls and Gerard J. Milburn, Quantum Optics (2008, 1994 Springer-Verlag Berlin Heidelberg) 2nd Edition, (2007).